Ultrathin Limit on the Anisotropic Superconductivity of Single-Layered Cuprate Films

Feng Ran(冉峰)[1,2], Pan Chen(陈潘)[1], Dingyi Li(李丁艺)[1,2], Peiyu Xiong(熊沛雨)[1], Zixin Fan(樊子鑫)[1], Haoming Ling(凌浩铭)[1,2], Yan Liang(梁艳)[1], and Jiandi Zhang(张坚地)[1,2*]

[1]*Beijing National Laboratory for Condensed Matter Physics, Institute of Physics, Chinese Academy of Sciences, Beijing 100190, China*
[2]*School of Physical Sciences, University of Chinese Academy of Sciences, Beijing 100049, China*

(Received 6 December 2023; accepted manuscript online 16 January 2024)

Exploring dimensionality effects on cuprates is important for understanding the nature of high-temperature superconductivity. By atomically layer-by-layer growth with oxide molecular beam epitaxy, we demonstrate that $La_{2-x}Sr_xCuO_4$ ($x = 0.15$) thin films remain superconducting down to 2 unit cells of thickness but quickly reach the maximum superconducting transition temperature at and above 4 unit cells. By fitting the critical magnetic field ($\mu_0 H_{c2}$), we show that the anisotropy of the film's superconductivity increases with decreasing film thickness, indicating that the superconductivity of the film gradually evolves from weak three- to two-dimensional character. These results are helpful to gain more insight into the nature of high-temperature superconductivity with dimensionality.

DOI: 10.1088/0256-307X/41/2/027401

Cuprates have attracted a great deal of attention since the discovery of their superconductivity in 1986,[1] which exhibit intensive novel physical properties, such as the highest critical temperature (T_c) for superconductivity at ambient pressure,[2] pseudogaps,[3,4] and strange metal state.[5–7] At present, understanding the mystery of high-T_c superconductivity has yet to be successful regardless of many attempts contributed. For cuprate superconductors, the inherently layered structures lead to the presence of strong in-plane to out-of-plane anisotropy. It is well known that the superconductivity of cuprates probably originates from the CuO_2 layer, but the role of the couplings between different CuO_2 layers in superconductivity, which are complex and varies with different cuprate structures, is still far from clarity, thus greatly impeding the understanding of high-T_c superconductivity mechanism. Therefore, creating two-dimensional cuprates without correlations between different CuO_2 layers is urgently needed to gain more insight into the nature of high-T_c superconductivity.

$La_{2-x}Sr_xCuO_4$, one of the first cuprate superconductors discovered, exhibits a simple layered crystal structure (K_2NiF_4-type) with alternatively stacked charge reservoir layers [(La/Sr)O] and superconducting CuO_2 layer in the c-axis direction. It has the highest T_c of about 40 K by tuning the doping concentration of Sr.[8] In this Letter, we present an atomically controlled synthesis of high-quality $La_{1.85}Sr_{0.15}CuO_4$ (LSCO) films with nearly optimal doped Sr via oxide molecular beam epitaxy (OMBE). By measuring the temperature (T) dependence of electric transport of the films with or without an external magnetic field, we reveal that films maintain superconducting and hold bulk-like T_c until the film thicknesses is below 2 unit cells (u.c.) and 4 u.c., respectively. The superconductivity in LSCO film transforms from three-dimensional (3D) to two-dimensional (2D) behavior with reducing films thickness. Through fitting the in-plane (parallel) and out-of-plane (perpendicular) upper critical fields of superconductivity, we demonstrate that the in-plane to out-of-plane anisotropy of superconductivity is enhanced as the film thickness is below $\sim$9 u.c., providing a signature of the 3D to 2D crossover of superconductivity.

We have grown crystalline LSCO films with different thicknesses on $LaSrAlO_4$ (LSAO) (001) substrates in atomically layer-by-layer manner via OMBE. LSAO is one of most suitable substrates for growing LSCO due to the similar tetragonal symmetry with small lattice mismatch (i.e., only about 0.5% with compressive strain to the LSCO films, see a schematic view in the inset of Fig. 1). The details about the film growth as well as the structural and property characterization are given in the Supplemental Material.

Figure 1(a) displays the sheet resistance versus temperature [$R_s(T)$] for LSCO films with different thicknesses grown on LSAO (001). It can be seen that the films exhibit a superconducting ground state when the LSCO film thickness is above 2 u.c., while there is a superconductor-to-insulator like transition with a critical thickness within 2 u.c. From the $R_s(T)$ curves of the superconducting samples, the linear resistive behavior in the normal state (strange metal state) is clearly observed, which is consistent with earlier findings.[5–7] In order to quantitatively compare the variation of superconductivity with film thickness, Fig. 1(b) summarizes the film thickness dependence of T_c, where T_c is defined as the temperature at which the resistance drops to half the normal-state resistance $R_{s,N}$ (the mean-field-theoretic transition temperature). It is found that the T_c values of LSCO films with the thickness above 4 u.c. are almost the same as the optimally doped bulk material. On the other hand, the film with the thickness below 4 u.c. decreases its T_c with decreas-

*Corresponding author. Email: jiandiz@iphy.ac.cn
© 2024 Chinese Physical Society and IOP Publishing Ltd

ing film thickness and exhibits no superconductivity below 2 u.c. The inset of Fig. 1(b) shows the $R_s(T)$ curve of a 2.0 u.c. LSCO film with a clear upward warping behavior of the resistance before the film enters the superconducting state, a behavior that has also been observed in underdoped $La_{2-x}Sr_xCuO_4$. Such a phenomenon is likely due to the weak localization effect or the effect of the different lattice distortions of the CuO_2 planes from the bulk material. In our experiments, it is possible that this is a critical state for the superconducting-insulating transition. [9–13]

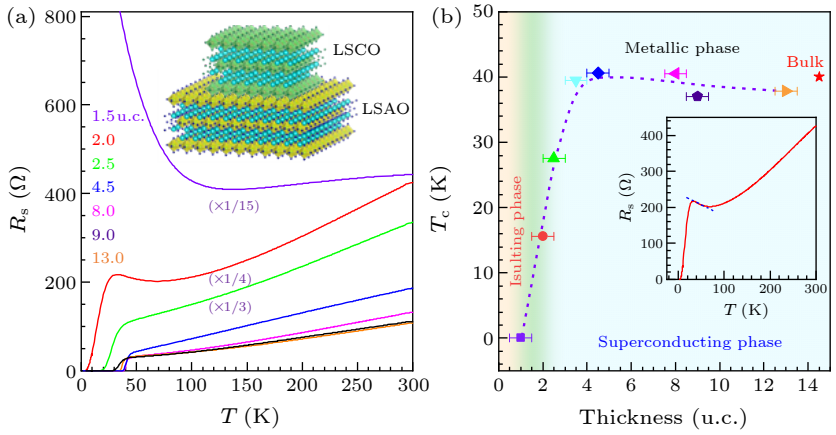

Fig. 1. Characterization of the superconducting properties: (a) T-dependence of in-plane sheet resistance R_s for LSCO thin films grown on LSAO (001) with different film thicknesses. (b) Thickness dependence of T_c, where T_c is defined as the temperature at which the resistance drops to half the normal state resistance. The dashed line is a guide to the eyes. The bulk T_c is also given for comparison. False-color regions schematically represent different phases of the films, while the dark green region marks the access region of the superconducting-insulating transition. Inset: $R_s(T)$ curve of a 2.0 u.c. LSCO film. Before entering the superconducting state, the $R_s(T)$ curve has a pronounced upturn behavior, which could be an intermediate state in the superconducting-insulating transition.

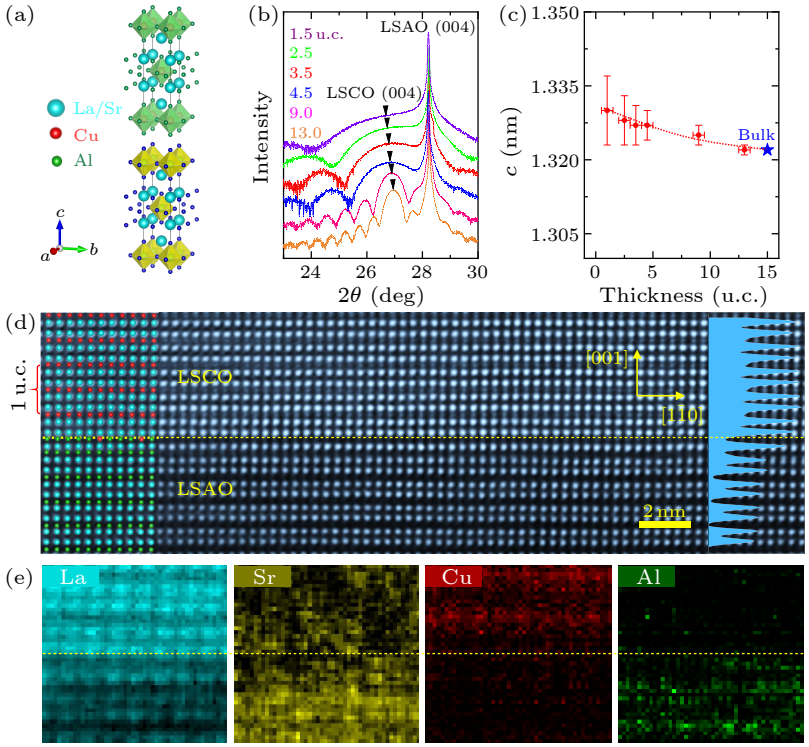

Fig. 2. Structural and compositional characterization: (a) Schematic unit-cell structures of $La_{2-x}Sr_xCuO_4$ and $LaSrAlO_4$, respectively. (b) The $2\theta/\omega$ XRD patterns of LSCO films with different thicknesses. (c) The c-axis lattice constants for the films with different thicknesses. The error bars are given according to the FWHM of the LSCO (004) peak. The bulk value is given for comparison. (d) Atomic-resolution HAADF-STEM image (HAADF: high-angle annular dark field) from a region near the interface of a 9.0 u.c. The LSCO film on LSAO taken along the [110] direction. The structural model is shown on the left and the inset on the right is the corresponding image intensity profile across the LSCO/LSAO interface. (e) Atomically resolved elemental maps of La, Sr, Cu, and Al across the interfaces by the electron-energy-loss spectroscopy. The position of the interface is marked by the yellow dash lines.

In order to confirm the variation of the lattice constants of LSCO films with film thickness and to determine whether there is strain release in the films, we performed x-ray diffraction (XRD) characterization of LSCO films with different thicknesses. Figure 2(a) displays the unit-cell tetragonal structures of both $La_{2-x}Sr_xCuO_4$ and LSAO, respectively. Figure 2(b) shows the XRD results of LSCO films with different thicknesses, and a larger scan range of XRD results are given in the Supplemental Material (see Fig. S2). The presence of only LSCO and LSAO diffraction peaks in the XRD results indicates that the grown LSCO films are highly oriented and free from other secondary or impurity phase. Kiessig fringes around the LSCO (004) diffraction peak indicates that the grown LSCO film has a very flat surface and interface with the substrate. At the same time, based on the position of the Kiessig fringes we can determine the thickness of the film,[14,15] which is consistent with the thickness of the film obtained by reflection high-energy electron diffraction oscillations during our growth. As shown in Fig. 2(c), the lattice constant c determined from the LSCO (004) diffraction peak increases slightly with decreasing film thickness, which is caused by the effects of the increased substrate-induced compressed strain as well as the possibly increased oxygen vacancies in the film as the LSCO thickness decreases. The presence of such effects is likely associated with the non-superconducting behavior in 1 u.c. LSCO films discussed below.

Our scanning transmission electron microscopy (STEM) imaging and spectroscopy reveal the well-ordered lattice structure of the grown LSCO films with atomically sharp interface with LSAO substrate. Figure 2(d) presents an atomically resolved STEM high-angle annular dark-field image from a region near the interface of LSCO/LSAO for a 9.0 u.c. LSCO film, where the intensity is nearly proportional to the square of the atomic number ($\sim Z^2$). It is clear that the film follows the tetragonal lattice structure of the substrate with atomically sharp interface. As shown in the atomically resolved intensity profile, the substrate is mainly terminated with AlO_2 layer, though the step effect in the STEM image and also possible minor single-layer Cu-Al intermixture result in an evolution of the intensity profile across the interface. Therefore, the initial layer grown on the AlO_2-terminated LSAO substrate is La/Sr–O layer and then followed by layer-by-layer growth of the LSCO film. Such interface and film structures are further validated by the electron-energy-loss spectroscopy elemental maps for La, Sr, Al, and Cu, as shown in Fig. 2(e).

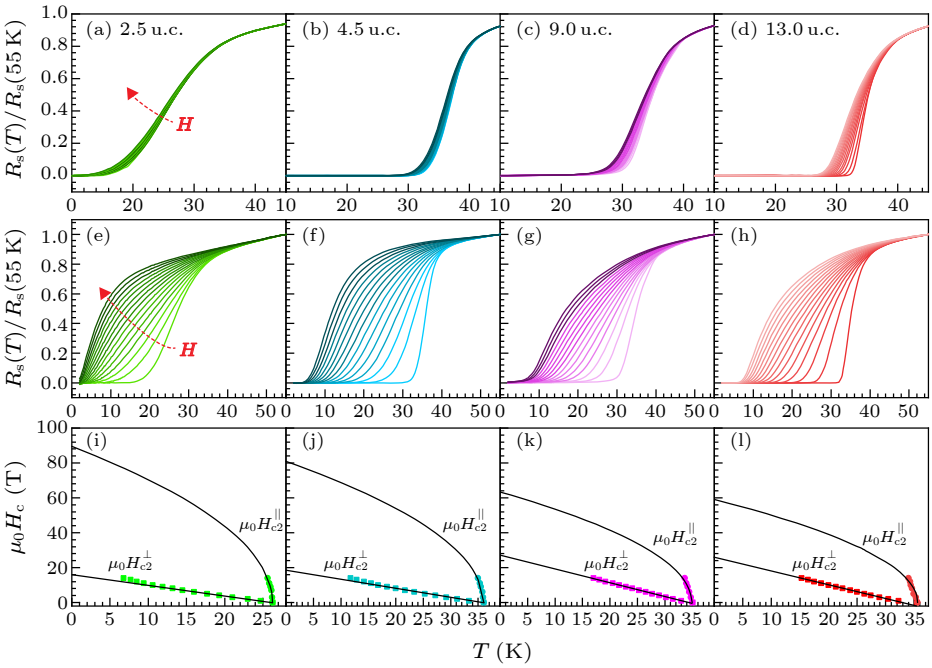

Fig. 3. Transport behavior under magnetic fields: $R_s(T)$ normalized to $R_s(T = 55\,K)$ of 2.5, 4.5, 9.0, and 13.0 u.c. LSCO films in magnetic fields (a)–(d) parallel and (e)–(h) perpendicular to the surface. (i)–(l) T-dependence of the upper critical field parallel ($\mu_0 H_{c2}^{||}$) and perpendicular ($\mu_0 H_{c2}^{\perp}$) to the surface for the corresponding films, where the upper critical field extracted from the half of normal-state resistance. The solid curves for $\mu_0 H_{c2}^{\perp}$ are the fitting results to the Ginzburg–Landau theory while for ($\mu_0 H_{c2}^{||}$) are the fitting results to Tinkham's model.

To investigate the thickness dependence of superconducting properties of LSCO films, we performed magnetic transport measurements on the films with different thicknesses by applying magnetic fields both parallel and perpendicular to the a–b plane, and the results are shown in Fig. 3. Figures 3(a)–3(d) and 3(e)–3(h) show the normalized resistance versus temperature curves for 2.5, 4.5, 9.0, and 13.0 u.c. LSCO films under the application of in-plane (parallel) and out-of-the plane (perpendicular) to the film surface magnetic fields of 0–14 T, respectively. As can be seen from Figs. 3(a)–3(h), LSCO, as a weak three-dimensional superconductor, exhibits significant enhance-

ment of the in-plane to out-of-the-plane anisotropy in the upper critical fields with decreasing film thickness.

Figures 3(i)–3(l) display the upper critical field parallel ($\mu_0 H_{c2}^{\parallel}$) and perpendicular ($\mu_0 H_{c2}^{\perp}$) to the surface for the corresponding films shown in Figs. 3(a)–3(h), which were extracted from the half of normal-state resistances. Clearly, these upper critical fields show strong in-plane to out-of-plane anisotropy which is enhanced with reducing film thickness. In particular, $\mu_0 H_{c2}^{\perp}$ shows a linear relationship with temperature, which is well described by the Ginzburg–Landau (G-L) theory for 2D superconductors [see the solid lines in Figs. 3(i)–3(l)] [16–18]

$$\mu_0 H_{c2}^{\perp}(T) = \frac{\phi_0}{2\pi[\xi_{GL}(0)]^2}\left(1 - \frac{T}{T_c}\right),$$

where $\xi_{GL}(0)$ is the G-L coherence length at $T = 0\,\mathrm{K}$, and ϕ_0 is the magnetic flux quantum.

The upper critical field is so large in the parallel direction that we were only able to obtain it in a narrow temperature range around T_c in our experiments, which makes it difficult to determine precisely the T-dependence of the upper critical field [see Figs. 3(i)–3(l)]. On the other hand, we can adopt the well-established models for 2D superconductors to estimate the T-dependence behavior. First, we fitted the upper critical field in the parallel direction $\mu_0 H_{c2}^{\parallel}(T)$ using Tinkham's model, [18–20]

$$\mu_0 H_{c2}^{\parallel}(T) = \frac{\sqrt{12}\phi_0}{2\pi\xi_{GL}(0)d_{SC}}\left(1 - \frac{T}{T_c}\right)^{1/2},$$

where d_{SC} is the superconducting thickness. Tinkham's model can describe the relationship between the parallel upper critical field and temperature under 2D superconductivity. The solid curves in Figs. 3(i)–3(l) present the fitting results with different film thicknesses using Tinkham's model to fit $\mu_0 H_{c2}^{\parallel}$ and to compare with the results of $\mu_0 H_{c2}^{\perp}$.

To avoid model dependence on the issue of such ultrathin film superconductivity, we have also analyzed our data by applying the Werthamer–Helfand–Hohenberg (WHH) theory, [21–24] which can account for the effects of both orbital and paramagnetic limitation. In the WHH theory, the zero-temperature upper critical field can be expressed as

$$H_{c2}(0) = -\alpha T_c \frac{dH_{c2}(T)}{dT}|_{T=T_c},$$

where α is the purity factor given by 0.693 and 0.73 for superconductor in the dirty and clean limits, respectively. Since $\mu_0 H_{c2}^{\parallel}$ shows a linear asymptotical behavior as $T \to T_c$, we used the linear slope value in the vicinity of T_c to yield the value of $dH_{c2}^{\parallel}(T)/dT|_{T=T_c}$ for different films, such that we can also give an estimate of the zero-temperature upper critical field by the WHH theory.

The fitting results of zero-temperature upper critical field to the three different models are summarized in Table 1. Though the extracted upper critical field values at $T = 0\,\mathrm{K}$ are model dependent, their thickness dependence is identical: the anisotropy of the film's superconductivity increases with decreasing film thickness, demonstrating that the superconductivity of the film gradually evolves from weak 3D to 2D character.

Table 1. Extrapolated upper critical field $\mu_0 H_{c2}$ values at $T = 0\,\mathrm{K}$ obtained by fitting to the Ginzburg–Landau theory, Tinkham's theory and the Werthamer–Helfand–Hohenberg theory, as well as the anisotropy index γ_1 and γ_2 (see the definition in the text) for different thicknesses of the films.

Thickness (u.c.)	T_c (K)	$\mu_0 H_{c2}^{\perp}(0)$ (T) (G-L theory)	$\mu_0 H_{c2}^{\parallel}(0)$ (T) (Tinkham's theory)	$\mu_0 H_{c2}^{\parallel}(0)$ (T) (WHH theory)	γ_1	γ_2
2.5	26.3	16.2	89.7	410	5.54	25.31
4.5	36	18.7	81	330	4.33	17.65
9.0	35	27.3	63.4	261	2.32	9.56
13.0	35.6	26.5	59	213	2.23	8.03

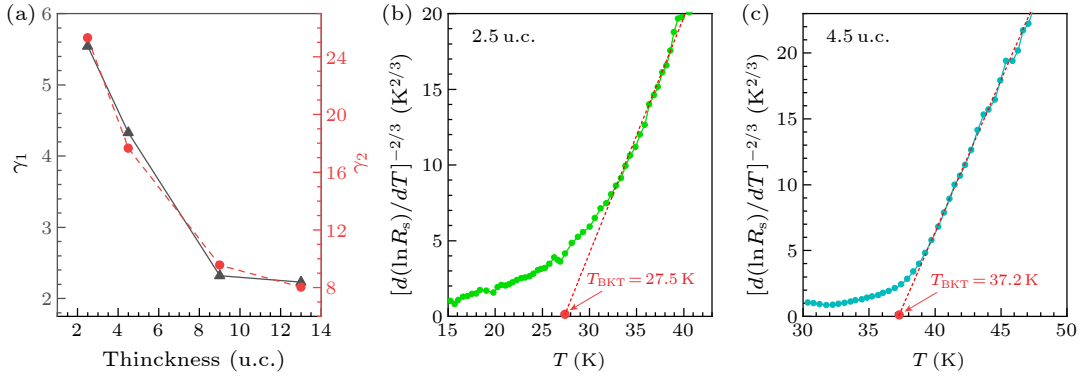

Fig. 4. Analyzed results the two-dimensional-like behavior: (a) Thickness-dependence of anisotropy index γ_1 and γ_2 (see the definition in the text) of LSCO films. (b) and (c) Plots of $[d(\ln R_s)/dT]^{-2/3}$ versus temperature for 2.5 and 4.5 u.c. films. The red line is the fitted curve and red arrows indicate Berezinskii–Kosterlitz–Thouless-like transition temperatures.

To quantitatively describe the variation of LSCO superconducting anisotropy with film thickness, we define the anisotropy index $\gamma = H_{c2}^{\parallel}/H_{c2}^{\perp}$. Here, γ_1 and γ_2, i.e., the values of γ based on ratio of $H_{c2}^{\parallel}$ fitted from the Tinkham model and the WHH theory to $H_{c2}^{\perp}$ derived from the G-L theory, respectively, are given in Table 1. As illustrated in Fig. 4(a), both γ_1 and γ_2 exhibit an identical thickness dependence, regardless having different values extracted from the fitting to different theoretical models. This clearly shows that the variation of LSCO anisotropy with thickness is independent of the theoretical fit, and that the enhancement of the anisotropy with reducing thickness is intrinsic 3D to 2D crossing behavior of superconductivity.

It is known that the Berezinskii–Kosterlitz–Thouless (BKT) phase transition,[25–28] at which vortex–antivortex pairs unbind is a signature for 2D-like superconductivity, in 2D superconductors is demonstrated by the T-dependence of the resistance via $R_{\rm s}(T)$ given by the Halperin–Nelson formula[26,29,30]

$$R_{\rm s}(T) = R_0 \exp\Big[-b\Big(\frac{T}{T_{\rm BKT}} - 1\Big)^{-\frac{1}{2}}\Big],$$

where R_0 and b are material parameters, and $T_{\rm BKT}$ is the BKT transition temperature.

As shown in Figs. 4(b) and 4(c), the $R_{\rm s}(T)$ data obtained from 2.5 u.c. and 4.5 u.c. LSCO films are consistent with the BKT-like behavior of 2D superconductors. Based on the fitting results, we obtain the BKT phase transition temperatures $T_{\rm BKT}$ of 27.5 K and 37.2 K for 2.5 and 4.5 u.c. films, and the corresponding maximum zero-resistance temperatures ($T_{\rm c0}$) are 20 K and 37 K, respectively, which indicates that the superconducting transitions of 2.5 u.c. and 4.5 u.c. films are consistent with that of a 2D superconducting film.

In summary, we have investigated the variation of superconductivity with thickness in ultrathin LSCO films by using atomically layer-by-layer OMBE growth and found that superconductivity disappears only when the LSCO thickness decreases below 2 u.c., in the middle of which there is likely insulator to superconductor crossover driven by the film thickness. Extrapolation from the fitting of the transport results under magnetic field indicates that the superconductivity of LSCO films undergoes a 3D to 2D transition with decreasing thickness, which is manifested as an enhancement of the superconducting anisotropy and consistent with BKT-like behavior in $R_{\rm s}(T)$ for the films in ultrathin limit. Our results bring new opportunities for understanding the unconventional superconductivity of cuprates in reduced dimensionality.

Acknowledgments. This work was supported by the National Key Research and Development Program of China (Grant No. 2022YFA1403000), and the National Natural Science Foundation of China (Grant No. 12250710675).

References

[1] Bednorz J G and Müller K A 1986 *Z. Phys. B* **64** 189
[2] Schilling A, Cantoni M, and Ott H R 1993 *Nature* **363** 56
[3] Ding H, Yokoya T, Campuzano J C, Takahashi T, Randeria M, Norman M R, Mochiku T, and Giapintzakis J 1996 *Nature* **382** 51
[4] Vishik I M 2018 *Rep. Prog. Phys.* **81** 062501
[5] Božović I, He X, and Bollinger A T 2016 *Nature* **536** 309
[6] Gurvitch M and Fiory A T 1987 *Phys. Rev. Lett.* **59** 1337
[7] Jin K, Butch N P, Kirshenbaum K, and Greene R L 2011 *Nature* **476** 73
[8] Tarascon J M, Greene L H, McKinnon W R, and Geballe T H 1987 *Science* **235** 1373
[9] Fisher M P A 1990 *Phys. Rev. Lett.* **65** 923
[10] Bollinger A T, Dubuis G, Yoon J, Pavuna D, and Božović I 2011 *Nature* **472** 458
[11] Schneider R, Zaitsev A G, and Löhneysen H v 2012 *Phys. Rev. Lett.* **108** 257003
[12] Meyer T L, Jiang L, Park S, and Lee H N 2015 *APL Mater.* **3** 126102
[13] Cieplak M Z, Berkowski M, Guha S, Cheng E, Vagelos A S, Rabinowitz D J, Wu B, and Lindenfeld P 1994 *Appl. Phys. Lett.* **65** 3383
[14] Miller A M, Lemon M, Choffel M A, Rich S R, and Johnson D C 2022 *Z. Naturforsch.* **77** 313
[15] Kiessig H 1930 *Naturwissenschaften* **18** 847
[16] Kozuka Y, Kim M, Bell C, Kim B G, and Hwang H Y 2009 *Nature* **462** 487
[17] Hsu J W P and Kapitulnik A 1992 *Phys. Rev. B* **45** 4819
[18] Saito Y, Kasahara Y, Ye J, and Nojima T 2015 *Science* **350** 409
[19] Tinkham M 1963 *Phys. Rev.* **129** 2413
[20] Tinkham M and Emery V 1996 *Phys. Today* **49** 74
[21] Maki K 1966 *Phys. Rev.* **148** 362
[22] Helfand E and Werthamer N R 1966 *Phys. Rev.* **147** 288
[23] Werthamer N R and Hohenberg P C 1966 *Phys. Rev.* **147** 295
[24] Yang P T, Liu Z Y, Chen K Y, Liu X L, Zhang X, Yu Z H, Zhang H, Sun J P, Uwatoko Y, Dong X L, Jiang K, Hu J P, Guo Y F, and Cheng J G 2022 *Nat. Commun.* **13** 2975
[25] Beasley M R and Orlando T P 1979 *Phys. Rev. Lett.* **42** 1165
[26] Guo J, Zhou Y, Huang C, Cai S, Sheng Y, Gu G, Yang C, Lin G, Yang K, Li A, Wu Q, and Sun L 2020 *Nat. Phys.* **16** 295
[27] Kosterlitz J M and Thouless D J 1973 *J. Phys. C: Solid State Phys.* **6** 1181
[28] Berezinskiĭ V L 1972 *Sov. Phys. JETP* **34** 610
[29] Halperin B I and Nelson D R 1979 *J. Low Temp. Phys.* **36** 599
[30] Reyren N, Thiel S, Caviglia A D, Kourkoutis L F, Hammerl G, Richter C, Schneider C W, Kopp T, Rüetschi A S, Jaccard D, Gabay M, Muller D A, and Mannhart J 2007 *Science* **317** 1196